

Cite this: *Chem. Commun.*, 2017, 53, 7521Received 1st June 2017,
Accepted 12th June 2017

DOI: 10.1039/c7cc04242f

rsc.li/chemcomm

Tuning the photocatalytic activity of bismuth wolframate: towards selective oxidations for the biorefinery driven by solar-light†

Rosaria Ciriminna,^a Riccardo Delisi,^a Francesco Parrino,^b Leonardo Palmisano^b and Mario Pagliaro^b

The sol-gel entrapment of nanostructured Bi_2WO_6 enhances the activity and the selectivity of the short-gap semiconductor in the sunlight-driven photo-oxidation of *trans*-ferulic and *trans*-cinnamic acid dissolved in water with air as the primary oxidant. Valuable products such as vanillin, benzaldehyde, benzoic acid and vanillic acid are obtained. This provides the proof of concept that photocatalysis could be a promising technology in tomorrow's solar biorefineries.

The aerobic oxidation of *trans*-ferulic acid (3-(4-hydroxy-3-methoxyphenyl)-2-propenoic acid) (1, Fig. 1) dissolved in water at room temperature in the presence of a suspension of catalytic amounts of nanostructured Bi_2WO_6 in the absence of light affords vanillic acid (4-hydroxy-3-methoxybenzoic acid) (3, Fig. 1) in high yield (60%).¹ Vanillic acid is a valued fragrance and flavoring agent with several beneficial effects due to its chemopreventive, hepatoprotective and cardioprotective activity,² and a global market in various application areas exceeding 200 million dollars.³ The reaction is important because the acid is a precursor of vanillin, one of the most important and expensive flavouring compound in the world (about 2400 dollars per kilogram for the natural product).⁴ Due to its small bandgap (2.7 eV), Bi_2WO_6 photocatalytically mediates the synthesis of chemicals and fuels under visible light, often with remarkable selectivity.⁵ When light is excluded, the adsorbed *trans*-ferulic acid molecules react with the $\text{W}=\text{O}$ active catalytic centres, whose concentration, among all possible bismuth tungstates, reaches a maximum in the Bi_2WO_6 phase.¹ However, when the visible-light conversion of *trans*-ferulic acid dissolved in water is carried out in an O_2 saturated atmosphere using the same flower-like Bi_2WO_6 , the former biophenol abundant in plants

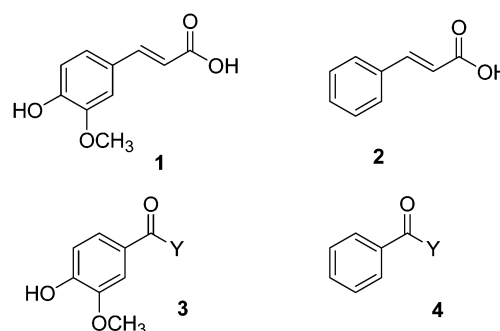


Fig. 1 Chemical structures of *trans*-ferulic acid (1), *trans*-cinnamic acid (2), vanillin (3, Y = H), vanillic acid (3, Y = OH), benzaldehyde (4, Y = H), and benzoic acid (4, Y = OH).

where it exerts numerous biological activities⁶ is first converted in small yield (*ca.* 1%) into vanillin (after 1 h) and then entirely mineralized into CO_2 .

Following promising findings applied to the conversion of glycerol into dihydroxyacetone,⁷ and aiming at finding a way to enhance the Bi_2WO_6 selectivity in the partial oxidation of phenolics of relevance to the bioeconomy, we entrapped flower-like Bi_2WO_6 in two different silica-based ceramic matrices. The resulting photocatalysts were used in the oxidation of *trans*-ferulic and *trans*-cinnamic acid (2, Fig. 1) under visible light and in the presence of different O_2 concentrations (0%, 20%, and 100% in the headspace).

All reactants, except the catalysts, were purchased from Sigma-Aldrich and used as received. Bi_2WO_6 was synthesized from $\text{Bi}(\text{NO}_3)_3 \cdot 5\text{H}_2\text{O}$ and $\text{Na}_2\text{WO}_4 \cdot 2\text{H}_2\text{O}$ via a well known hydrothermal route in which careful control of the reaction time (8 h) affords the required flower-like Bi_2WO_6 microparticles.⁸ The XRD analysis (Fig. S1 in the ESI†) confirmed the formation of crystalline Bi_2WO_6 with the main patterns at $2\theta = 28^\circ$, 33° , 47° , and 56° . Analysis of the SEM and TEM images revealed the formation of the flower-like nanostructures.¹ The sol-gel entrapped Bi_2WO_6 catalysts were prepared using TEOS (tetraethylorthosilicate) and MTES (methyltriethoxysilane) as silica

^a Istituto per lo Studio dei Materiali Nanostrutturati, CNR, via U. La Malfa 153, 90146 Palermo, Italy. E-mail: mario.pagliaro@cnr.it

^b "Schiavello-Grillone" Photocatalysis Group, DEIM, Università degli Studi di Palermo, viale delle Scienze, 90128 Palermo, Italy. E-mail: francesco.parrino@unipa.it

† Electronic supplementary information (ESI) available. See DOI: 10.1039/c7cc04242f

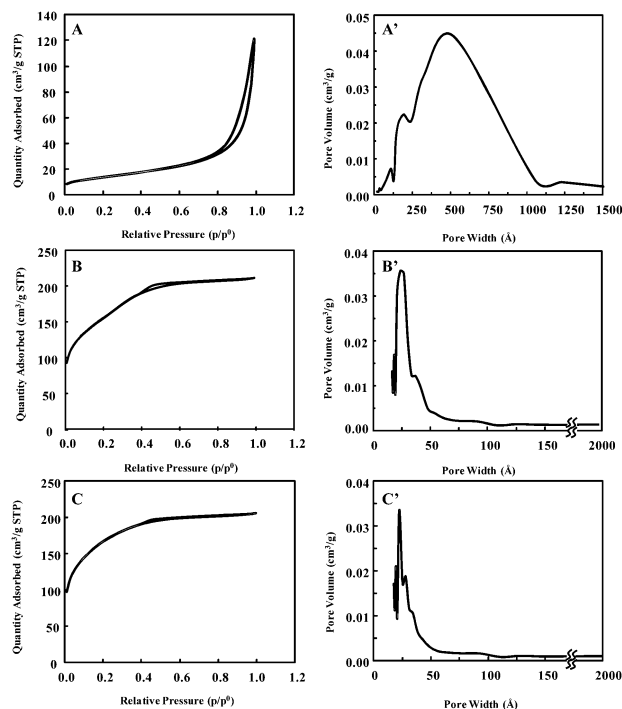


Fig. 2 N₂ adsorption–desorption isotherms (A–C), pore size distribution (A'–C') of the samples: pure Bi₂WO₆ (A and A'), SiliaSun Me0% (B and B'), and SiliaSun Me10% (C and C').

precursors (see ESI[†]). SEM and TEM analyses of the resulting embedded methylated (SiliaSun Me10%) and non-methylated (SiliaSun Me 0%) photocatalysts (see Fig. S2 and S3 in the ESI[†]) confirm that even though the flower-like superstructure of the original Bi₂WO₆ is destroyed, crystalline Bi₂WO₆ is entrapped in an amorphous glassy silica or an organosilica matrix, an encapsulating shell clearly distinguished.

The nitrogen adsorption–desorption isotherms at –196 °C and the pore size distribution for all of the samples are displayed in Fig. 2. The type IV isotherm of pure Bi₂WO₆, according to the De Boer classification,⁹ is associated with capillary condensation taking place in mesopores (see the average pore size of Bi₂WO₆ of 15.5 nm, Table 1). The initial segment of the isotherm at low relative pressure values may be attributed to monolayer–multilayer adsorption. Thereafter, the almost linear middle section indicates that monolayer coverage is complete and multilayer adsorption takes place. The shape of the hysteresis loop (type H1) suggests the presence of spherical particles arranged in a fairly uniform way with facile pore connectivity. Although the hysteresis takes place at a relatively high pressure (between 0.8 and 1.0),

Table 1 BET (Brunauer–Emmet–Teller) specific surface area (SSA), particle size, total pore volume (V_p), and average pore diameter (D_p) of the used samples

	SSA [m ² g ⁻¹]	Particle size [nm]	V _p [cm ³ g ⁻¹]	D _p [nm]
Bi ₂ WO ₆	48.2	124.4	0.187	15.5
SiliaSun Me0%	538.2	11.1	0.326	2.4
SiliaSun Me10%	560.2	10.7	0.318	2.3

confirming the presence of mesopores, the shape of the adsorption branches at p/p_0 close to 1 is somewhat similar to type II isotherm, indicating the presence of macropores, too.^{10,11}

Indeed, the pore size distribution curve shows a broad distribution of up to 1000 Å centered at about 500 Å, with an average particle size of 124.4 nm (Table 1). The isotherms of the SiliaSun catalysts are very similar and may be associated with type I isotherm typical for microporous solids. The pore diameter indeed is slightly greater than 2 nm for both SiliaSun samples with a relatively small external surface, and a large inner surface area typical of silica sol–gels which is 11–12 times greater than that of Bi₂WO₆ with a correspondingly smaller average particle size (Table 1). Although the reported pore size of the SiliaSun samples is at the upper limit of the size reported in the literature for micropores, the shape of the isotherms shown in Fig. 2B and C is ascribed to microporous solids. The presence of a small, almost horizontal hysteresis loop associated with the H4 type isotherm indicates the presence of narrow slit-like pores and particles with internal voids of irregular shape. For both sol–gel entrapped catalysts, the pore size distribution curves show a narrow distribution of up to 50 Å centered at about 25 Å.

The oxidation reactions were carried out in a tightly closed reaction tube with 10 mL of an aqueous solution (0.5 mM) of a substrate and 1.5 g L⁻¹ of a catalyst, either as such or sol–gel entrapped. The tube placed in a water bath was inserted into an air cooled solar light simulator (Solar Box, CO.FO.ME.GRA., Milan, Fig. S4 in the ESI[†]) equipped with a 1500 W Xenon lamp irradiating the reaction mixture with simulated solar light (no UV filter). The temperature of the water bath reached 60 °C and did not further change until the light was kept on. The samples withdrawn from the reaction mixture were filtered off through a nylon filter (0.2 μm) prior to HPLC analysis. Solvents of HPLC grade were degassed prior to analysis. The total organic carbon (TOC) analysis was conducted using a Shimadzu TOC-5000A analyzer.

Preliminary experiments, in the presence of the SiliaSun samples, were performed in an O₂ atmosphere under otherwise similar experimental conditions. In this case, the conversion of the substrates was almost complete (above 90%) after 3 h of irradiation, but the selectivity towards the compounds of interest was unsatisfactory (*ca.* 3% for vanillic acid and *ca.* 2% for vanillin starting from ferulic acid; and *ca.* 6% for benzaldehyde and *ca.* 4% for benzoic acid starting from cinnamic acid) with CO₂ being the main oxidation product with both substrates. Notably, a negligible conversion of the substrate was obtained under a N₂ saturated atmosphere even after 6 h, confirming the central role played by O₂ in this kind of oxidation. Blank tests in the absence of light under the same experimental conditions did not show any activity after the same reaction time. The results in Table 2 were obtained by carrying out the reaction in the presence of air.

The latter results (see also Tables S1–S3 in the ESI[†]) show that, in each case, switching from O₂ to air significantly reduces the mineralization while affording the formation of vanillic acid and vanillin. The sol–gel entrapment of Bi₂WO₆ in the non-photo-active silica matrix reduces the overall conversion but doubles the selectivity to vanillic acid with respect to bare Bi₂WO₆ by dispersing the active Bi₂WO₆ phase and lowering the

Table 2 Conversion of ferulic acid in air under visible light over free and sol-gel entrapped Bi_2WO_6 . The figures are the average of the results obtained in three independent runs carried out under the same experimental conditions

Catalyst	Reaction time (h)	Ferulic acid conversion (%)	Vanillic acid selectivity (%)	Vanillin selectivity (%)
Bi_2WO_6	1	42	5.0	2.7
	2	78	13.7	4.1
	3	80	15.3	4.5
	6	86	15.6	4.9
SiliaSun Me0%	1	21	10.0	1.1
	2	36	30.0	1.2
	3	37	32.8	1.8
	6	59	26.0	2.0
SiliaSun Me10%	1	21	12.0	0.8
	2	31	38.5	2.1
	3	35	33.7	3.6
	6	61	31.0	4.1
TiO_2	1	93	—	1.2
	3	99	0.2	2.1

Reaction conditions: 10 mL aqueous substrate solution (0.5 mM), 1.5 g L^{-1} catalyst, Solar Box irradiation (Xe lamp, 1500 W, no UV filter), vigorous magnetic stirring.

overall oxidative capability of the photocatalysts. This trend is generally observed for similar systems.¹² Highlighting the remarkable effect of Bi_2WO_6 sol-gel encapsulation, the activity per mass of Bi_2WO_6 is higher in the embedded samples with respect to that of the bare photocatalyst. Indeed, the active Bi_2WO_6 phase constitutes only 10% of the weight of the SiliaSun samples. It is worth mentioning that comparable selectivity values of vanillic acid were obtained in the dark in the presence of bare Bi_2WO_6 .¹ However, while in the dark almost 90 h were required, under solar light irradiation the same selectivity and yield values were obtained in 3 h. Fig. 3A and B show the concentration of *trans*-ferulic acid during irradiation and the corresponding selectivity towards vanillic acid over pure Bi_2WO_6 and over the SiliaSun photocatalysts. Notably, the reduced conversion obtained for the embedded photocatalysts with respect to Bi_2WO_6 (Fig. 3A) translates into twice higher selectivity values (Fig. 3B). It is evident from Fig. 3B that the selectivity reaches a maximum and then decreases after a critical reaction time. This general trend is due to the competition for oxidation between the formed target compounds and the substrate molecules. For the sake of comparison, the oxidation of *trans*-ferulic acid was performed under the same experimental conditions in the presence of TiO_2 P25 (Evonik, Germany). In this case the substrate is almost completely oxidized after 1 h of irradiation and the selectivity towards the desired products is very poor, thus demonstrating the superior synthetic performance of the Bi_2WO_6 photocatalysts. Indeed, differently from TiO_2 mediated photo-oxidations, Bi_2WO_6 induced photocatalytic oxidation processes do not proceed through $\cdot\text{OH}$ radicals but *via* direct holes and *via* more selective peroxidic species including activated oxygen (*e.g.*, $\text{O}_2^{\cdot-}$).¹³⁻¹⁵

The commercial value of both vanillin and vanillic acid is so high that the hereby reported selectivity values are of practical interest. Notably, ferulic acid partial oxidation has been reported in the presence of TiO_2 in water under UV¹⁶ or visible

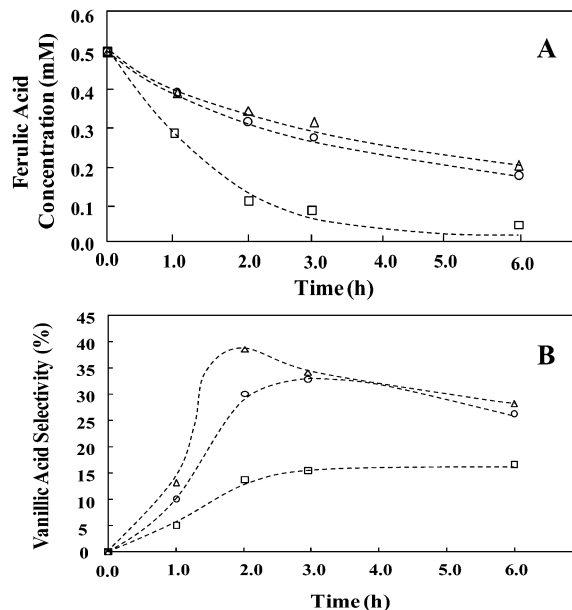


Fig. 3 Concentration of ferulic acid during irradiation time (A) and the corresponding selectivity values towards vanillic acid (B) for pure Bi_2WO_6 (\square), SiliaSun Me0% (\circ), and SiliaSun Me10% (Δ) photocatalysts in representative runs.

light¹⁷ irradiation. In the latter case, selective permeation of vanillin through a membrane strongly enhanced the selectivity of the process by continuously separating the product from the reaction medium, thereby efficiently preventing its further oxidation.¹⁸ This system allows us to both completely retain the photocatalytic powder into the reaction unit and to afford downstream highly pure (99.98%) crystals of vanillin.¹⁹ The application of the latter integrated system to the SiliaSun samples, which affords significantly higher yields of vanillic acid when compared to TiO_2 , is therefore promising.

The same selectivity trend was also observed in the oxidation of *trans*-cinnamic acid (Table 3 and Fig. S5 in the ESI[†]). Hence, while the reaction over a suspension of Bi_2WO_6 under O_2 resulted in complete mineralization after 3 h, the replacement of O_2 with air afforded a complete photocatalytic conversion into a mixture of benzoic acid and benzaldehyde in 6 h, with a predominance of benzoic acid (see Tables S1–S3 in the ESI[†]). Again, replacing Bi_2WO_6 with the SiliaSun catalysts alters both the activity and the selectivity of bismuth tungstate. Now, after 6 h a large amount of benzaldehyde is obtained along with unreacted substrate both in the original *trans*-configuration, and isomerized into the *cis*-form. Indeed, upon irradiation with visible light *trans*-cinnamic acid dissolved in water photochemically isomerizes into *cis*-cinnamic acid.²⁰

Similarly to what was observed with *trans*-ferulic acid, using the 10%-methylated SiliaSun catalyst slightly enhances the selectivity towards the aldehyde (by considering the figures at various reaction times), which now becomes the predominant reaction product (Table 3 and Fig. S4 in the ESI[†]). Indeed, the silica entrapment addressed the reaction selectivity to the aldehyde or the acid, depending on the affinity with the used substrate. For all of the runs TOC analysis confirmed a satisfactory carbon mass balance, indicating that no other

Table 3 Conversion of *trans*-cinnamic acid under visible light over free and sol-gel entrapped Bi₂WO₆. The figures are the average of the results obtained in three independent runs carried out under the same experimental conditions

Catalyst	Reaction time (h)	Cinnamic acid conversion (%)	Benzoic acid selectivity (%)	Benzaldehyde selectivity (%)
Bi ₂ WO ₆	1	77	5.5	7.4
	2	92	8.5	8.5
	3	98	13.6	10.3
	6	100	20.1	13.4
SiliaSun Me0%	1	28	1.2	3.7
	2	37.7	1.5	8.0
	3	59.5	2.9	9.7
	6	73	6.5	16.7
SiliaSun Me10%	1	23	2.7	6.0
	2	55	2.8	8.0
	3	79	2.9	11.0
	6	82	6.4	17.1
TiO ₂	1	87	4.4	1.50
	3	99	3.8	2.4

Reaction conditions: 10 mL aqueous substrate solution (0.5 mM), 1.5 g L⁻¹ catalyst, Solar Box irradiation (Xe lamp, 1500 W, no UV filter), vigorous magnetic stirring.

intermediates were produced during the reaction with the exception of CO₂ and the species detected by HPLC. Finally, to check for possible leaching of active Bi₂WO₆ reaction centres in solution, the solid catalyst was removed by filtration using a 0.20 μm nylon filter after 90 min (50% of total conversion). The filtrate monitored for activity within the subsequent 2 h showed no further reaction, indicating that no catalytically active species were present in the filtrate. Moreover, the filtrate analyzed by ICP-MS showed no presence of bismuth or tungsten, thereby excluding leaching of the insoluble Bi₂WO₆ or its derivatives. Further pointing to no changes in the catalyst structure upon reaction, the XRD analysis of the used photocatalysts revealed that in each case the crystal structure was not affected by the photocatalytic reaction. Furthermore, the conversion and selectivity values remained virtually unchanged after three reaction runs performed with the same catalyst filtered, washed with distilled water and reused as such in a subsequent reaction run. All these evidences indicate the catalytic nature of the reaction and the recyclability of the catalysts. In analogy to silica-supported TiO₂, in which the formation of Ti–O–Si linkages induces a remarkable optical modification ascribed to the electronic semiconductor support interaction,^{21,22} we propose a hypothesis that the sol-gel encapsulation of Bi₂WO₆ likely induces the formation of oxygen bridges between Si and W with different intermediate energy states. Indeed, the photoluminescence spectra of the SiliaSun Me0% catalyst⁷ display much lower intensity with respect to bare Bi₂WO₆, (see Fig. S6 in the ESI[†]), suggesting an interaction between silica and Bi₂WO₆ that markedly influences the spatial electron and hole transfer kinetics. This hypothesis may justify the observed high activity of the embedded samples even if they contain only 10% in weight of the optically active Bi₂WO₆ phase (see Fig. S7 in the ESI[†]).

In conclusion, we have discovered that *trans*-ferulic acid and *trans*-cinnamic acid dissolved in water can be selectively oxidized with significant yield into a mixture of valued acid and aldehyde derivatives (vanillic acid and vanillin, and benzoic acid and benzaldehyde, respectively) under simulated solar light irradiation over flower-like nanostructured Bi₂WO₆ and, even better, over the SiliaSun sol-gel entrapped forms. The sol-gel encapsulation of the photocatalyst significantly enhanced the selectivity towards the aldehyde or the acid, depending on the nature of the substrate. These findings could be relevant from both scientific and technological viewpoints. From the application viewpoint, in light of the forthcoming broad utilization of solar photocatalysis to chemical synthesis,²³ the robustness, low cost and highly porous nature of the sol-gel glassy catalyst make it ideally suited for continuous practical applications. Further experiments are ongoing on different substrates and different SiliaSun catalysts.

This article is dedicated to Professor David Avnir, eminent chemistry scholar at the Hebrew University of Jerusalem, on the occasion of his 70th birthday. We thank Prof. Yi-Jun Xu, Fuzhou University, for prolonged collaboration in this field of our researches.

References

- 1 R. Delisi, R. Ciriminna, F. Parrino, L. Palmisano, Y.-J. Xu and M. Pagliaro, *ChemistrySelect*, 2016, **1**, 626–629.
- 2 S. Kumar, P. Prahalathan and B. Raja, *Environ. Toxicol. Pharmacol.*, 2014, **38**, 643–652.
- 3 QY Research Reports, Global Vanillic Acid Industry 2015 Market Research Report, March 2015.
- 4 L. Lesage-Meessen, M. Delattre, M. Haon, J. F. Thibault, B. C. Ceccaldi, P. Brunerie and M. Asther, *J. Biotechnol.*, 1996, **50**, 107–113.
- 5 N. Zhang, R. Ciriminna, M. Pagliaro and Y.-J. Xu, *Chem. Soc. Rev.*, 2014, **43**, 5276–5287.
- 6 N. Kumar and V. Pruthi, *Biotechnol. Reprod.*, 2014, **4**, 86–93.
- 7 Y. Zhang, R. Ciriminna, G. Palmisano, Y.-J. Xu and M. Pagliaro, *RSC Adv.*, 2014, **4**, 18341–18346.
- 8 Y. Zhang, N. Zhang, Z.-R. Tang and Y.-J. Xu, *Chem. Sci.*, 2013, **4**, 1820–1824.
- 9 J. H. De Boer, *The Structure and Properties of Porous Materials*, Butterworths, London, 1958, p. 68.
- 10 S. W. Liu and J. G. Yu, *J. Solid State Chem.*, 2008, **181**, 1048–1055.
- 11 J. G. Yu, Q. J. Xiang, J. R. Ran and S. Mann, *CrystEngComm*, 2010, **12**, 872–879.
- 12 M. A. Lazar and W. A. Daoud, *RSC Adv.*, 2013, **3**, 4130–4140.
- 13 G. Scandura, R. Ciriminna, Y.-J. Xu, M. Pagliaro and G. Palmisano, *Chem. – Eur. J.*, 2016, **22**, 7063–7067.
- 14 S. Zhu, T. Xu, H. Fu, J. Zhao and Y. Zhu, *Environ. Sci. Technol.*, 2007, **41**, 6234–6239.
- 15 Y. Zhang and Y.-J. Xu, *RSC Adv.*, 2014, **4**, 2904–2910.
- 16 V. Augugliaro, G. Camera-Roda, V. Loddo, G. Palmisano, L. Palmisano, F. Parrino and M. A. Puma, *Appl. Catal., B*, 2012, **111–112**, 555–561.
- 17 F. Parrino, V. Augugliaro, G. Camera-Roda, V. Loddo, M. J. López-Muñoz, C. Márquez-Álvarez, G. Palmisano, L. Palmisano and M. A. Puma, *J. Catal.*, 2012, **295**, 254–260.
- 18 G. Camera Roda, V. Augugliaro, V. Loddo, G. Palmisano and L. Palmisano, EP2580182, 2016.
- 19 G. Camera-Roda, A. Cardillo, V. Loddo, L. Palmisano and F. Parrino, *Membranes*, 2014, **4**, 96–112.
- 20 F. Parrino, A. Di Paola, V. Loddo, I. Pibiri, M. Bellardita and L. Palmisano, *Appl. Catal., B*, 2016, **182**, 347–355.
- 21 H. Weiss, A. Fernandez and H. Kisch, *Angew. Chem., Int. Ed.*, 2001, **40**, 3825–3827.
- 22 M. Gärtner, V. Dremov, P. Müller and H. Kisch, *ChemPhysChem*, 2005, **6**, 714–718.
- 23 R. Ciriminna, R. Delisi, Y.-J. Xu and M. Pagliaro, *Org. Process Res. Dev.*, 2016, **20**, 403–408.